OPTIMAL SIZING OF AN AMMONIA PRODUCTION AND TRANSPORTATION SUPPLY CHAIN BASED ON RENEWABLE ELECTRICITY: COMPARISON BETWEEN PARAMETRIC STUDY AND COSTS-EMISSIONS BI-OBJECTIVE OPTIMIZATION

Cécile Diamantis[1]*, Alain Ruby[1], Pimprenelle Parmentier[1], Elise Le Goff[1]

[1]CEA, LITEN/DTCH.SSETI/LSET, Grenoble, France

*cecile.diamantis@cea.fr

ABSTRACT

Large-scale hydrogen production and transportation for power-to-power supply chain has gained in interest in the context of energy decarbonisation. Hydrogen can be carried in vessels, in various forms: liquefied hydrogen, ammonia, liquid organic carrier, among others. The production and the transport impact each other, and choices of technologies, sizes and control have to be optimized together. In this work, we present a MILP model of batch transportation included within a global MILP model which encompasses several appliances functioning together: a renewable electricity production, an electrolyser, energy and gas storages, ammonia as hydrogen carrier and a gas turbine. The MILP model optimizes sizing and control of the complete hydrogen supply chain, however it is costly to compute. We propose and combine two methods to reduce the number of integer variables for batch transportation: the template method and the time aggregation applied to transportation. The combination of these two methods reduces the computation time by 330 without losing results quality (gap lower than 0.7%). This computation time reduction enables to perform bi-objective optimization. A parametric study on carbon emissions and bi-objective optimization with an external loop to the MILP model are performed and compared in terms of total costs of the supply chain, carbon emissions and computation time.

1 INTRODUCTION

Large-scale hydrogen transportation for power-to-power supply chain has gained in interest, in a context of energy systems decarbonisation. Especially since Fukushima Daiichi accident, Japan has engaged in the research for a reliable and affordable source of CO_2-free energy. Hydrogen has been identified as one of the solutions to provide this energy. Kamiya, *et al.* (2015) studies this option with hydrogen produced from brown coal in combination with carbon dioxide capture and storage. Heuser *et al.* (2019) approaches the issue from a global perspective between Patagonia and Japan, and shows that 25% of the land would be necessary to produce hydrogen with wind power. With a simplified equation to model the number of required ships to ensure the deliveries, they show that the cost of transportation amounts to 25% of the total costs, whilst the liquefaction amounts to 10% of the total costs. This underlines the importance of transport optimization in supply chains. Hong *et al*. (2021) compares four options for hydrogen transportation by vessel: cyclohexane, liquid hydrogen, compressed hydrogen and liquid ammonia, to provide Japan with hydrogen from different parts of Asia. As mentioned in the review of Riera *et al* (2023), modelling and optimizing hydrogen transport remains not frequently addressed in the literature.

In this article, we present a comprehensive MILP (Mixed Integer Linear Problem) model of the entire hydrogen supply chain starting from the generation of electricity from both photovoltaic (PV) and wind turbine sources, to the delivery to consumers in Japan, this with a granularity of two hours. A detailed model leads to high computation times. To overcome this, we combine and test two methods to reduce the size of the problem without losing quality: the time-step aggregation method and the template

https://doi.org/10.52202/077185-0094

method. In most cases, time aggregation has been used for time series aggregation with the final objective to reduce energy system models complexity (Hoffman and al, 2020) (Cuisinier and al, 2021). In this paper, time aggregation is used only for one component of the supply chain (the vessels).

Section 1 presents the case study, a power-to-power supply chain between Australia and Japan with ammonia as hydrogen carrier. Section 2 presents the objective functions and the numerical tools used: Persee, an optimization tool developed by CEA (Cuisinier et al. 2022) to conduct techno-economic and environmental studies for multi-energies systems at different scales and the evolutionary algorithm NSGA III available in URANIE platform (Blanchard et al. 2019). Section 4 focuses on the transport modelling part, developed for Persee as well as the two aforementioned methods that were developed to drastically reduce the number of integer variables. The reduced computation time allows hybridizing the MILP model with a genetic algorithm (the open-source Uranie platform) to perform a cost-emission bi-objective optimization including non-linear contribution of ship sizes and number of ships. Section 5 presents the comparison of a parametric study on carbon emissions and the bi-objective optimization.

2 CASE STUDY PRESENTATION

2.1 Power-to-power supply chain between Australia and Japan

The case study consists in a power-to-power supply chain between Australia and Japan with the aim to decarbonize Japanese electricity system. Figure 1 presents the considered supply chain.

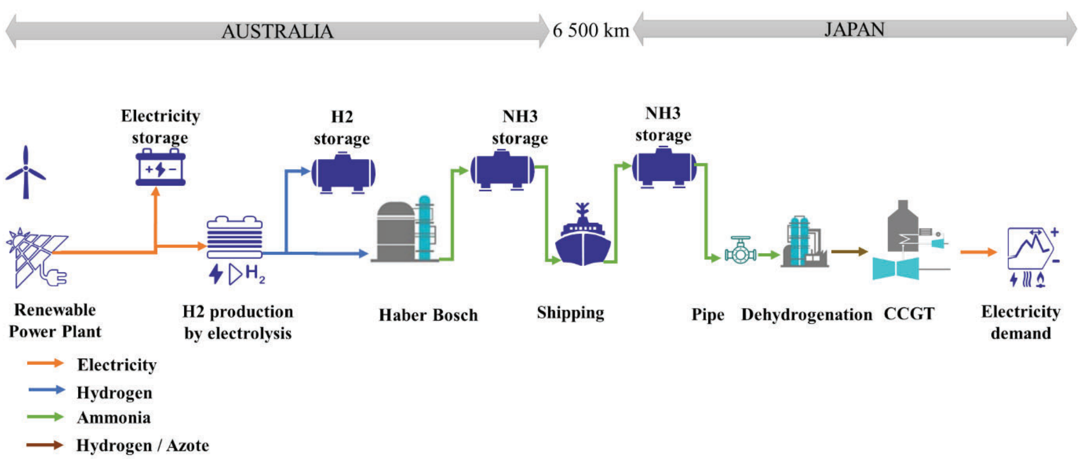

Figure 1 - Overview of the supply chain

In Australia, electricity produced by solar and wind power plants supplies electrolyzers. The resulting hydrogen allows producing ammonia through a Haber Bosh unit. All along the supply chain, electricity storage, hydrogen storage and ammonia storage allow to deal with the intermittency of the electricity production. Ammonia as hydrogen carrier is then used for overseas batch transportation. In Japan, the ammonia is dehydrogenated and the resulting hydrogen is fed in a CCGT to produce electricity.

The following hypotheses are considered:

- **Electricity production**:
  - Ensured by solar and wind power plants, of which the sizes ($\boldsymbol{S_{PV}}$) and ($\boldsymbol{S_{WP}}$) are variables of optimization. There is no grid connection.
  - Curtailment is possible up to 10% of the installed capacity.
  - The unitary power of solar and wind sources is provided for every two-hour interval throughout the year.
- **Hydrogen production and storage**:
  - Ensured by a Proton Exchange Membrane (PEM) electrolyzer, optimized in size ($\boldsymbol{S_E}$).
  - The electrolyzer has an efficiency of 65%.

https://doi.org/10.52202/077185-0094

- A compressor compresses hydrogen up to 200 bar with an electric consumption associated to the quantity compressed.
- The sizes of the H2 tank ($\boldsymbol{S_{TH2}}$) and compressor ($\boldsymbol{S_{CH2}}$) are optimized.

- **Ammonia production and storage:**
  - Haber-Bosch converts hydrogen and nitrogen to ammonia. Its size ($\boldsymbol{S_{HB}}$) is optimized.
  - The unit is flexible from 37% to 100% of maximum power, with no ramp limitations.
  - Ammonia storages, optimized in size, allow storage before and after transportation.
- **Transportation:**
  - Ammonia is transported by batches in vessels of fixed capacity(C). The total number of vessels ($\boldsymbol{S_{TR}}$) is optimized. The distance D between departure and arrival and the speed of a vessel sp allows to deduce a time $t_{aj} = \left\lceil \frac{D}{sp} \right\rceil$ to travel between departure and arrival.
  - A fraction of the transported ammonia is self-consumed by the vessels.
- **Electricity production and consumption in Japan:**
  - Ammonia is converted into hydrogen via dehydrogenation.
  - The CCGT converts the hydrogen into electricity with a given efficiency.
  - Electricity demand is stable over the year with 4 maintenance periods.
  - The consumption time series are provided for every two hours of the year.
  - Annual Electricity demand is about 5 660 GWh.

2.2 Specifics of the case study

The case study takes into account losses all along the supply chain (0.3 to 1% of the output stream for each component), GHG emissions linked to the construction of each component and linked to their operation. Another specificity of the case study lies in the optimization of the complete supply chain from PV and wind power plants to electricity production in Japan, including overseas batch transportation.

3 METHODOLOGY

3.1 Objective functions

We defined two objective functions. The first one is the minimization of total costs over 25 years, including investment and operation costs (1). The second one is the minimization of carbon emission over 25 years, including emissions linked to the construction of each component of the supply chain as well as emissions linked to their operation (2). Every modelled component is associated to a contribution in Capex and Opex, as well as a grey and direct emission of CO2.

The economic objective function (1) is the following:

$$Eco(\boldsymbol{s}, \boldsymbol{v}) = \sum_{i \in \mathcal{I}} \left[c_i (1 + o_i) * \boldsymbol{s_i} + \sum_{t \in \mathcal{Y}} p_{i,t} * \boldsymbol{v_{i,t}} \right] \tag{1}$$

For each component i of the system, the size $\boldsymbol{s_i}$ and the control $\boldsymbol{v_{i,t}}$ are optimized to minimize the economic function. Total costs are the considered economic indicators, consequently, we did not consider any discount factor. c_i is the unitary capex of i and o_i a unitary fixed opex per year.
The CO2 function (2) is computed on the same principle:

$$CO_2(\boldsymbol{s}, \boldsymbol{v}) = \sum_{i \in \mathcal{I}} \left[g_i * \boldsymbol{s_i} + \sum_{t \in \mathcal{Y}} d_{i,t} * \boldsymbol{v_{i,t}} \right] \tag{2}$$

With g_i the grey emission associated to the construction of the component i and d_i the direct emissions caused by the control over the year.

https://doi.org/10.52202/077185-0094

3.2 Multi-objective optimization with PERSEE software and URANIE platform

Mixed Interger Linear Programming (MILP) optimization has been largely used for hydrogen supply chains design and optimization since 2005 (Efthymiadou *et al* 2024), (Riera *et al* 2023). CEA has been developing since 2018 the PERSEE modelling software to conduct techno-economic and environmental studies (Cuisinier *et al*. 2022). PERSEE, based on a MILP formalism, optimizes sizing and operation at hourly (or two hours) time step, extrapolated to the project's lifetime (here 25 years). The objective function is the costs function described in 3.1 (1).

In order to include environmental impacts from grey emissions (i.e. manufacturing) or direct emissions (by combustion or operation) two options are possible:

- A parametric study on carbon emissions. The cost objective function is minimized under emissions constraints. An experience plan with increasing carbon constraints is built and allows obtaining sets of non-dominated solutions (i.e Pareto front).
- Using an external optimization loop to take into account the environmental objective function described in 3.1 (2). We chose to use evolutionary algorithm NSGA III available in URANIE platform (Blanchard *et al.* 2019). The Uranie platform, developed by CEA is an open-source software for optimization, meta-modelling and uncertainty analysis.

4 BATCH TRANSPORTATION SIMULATION

4.1 Transportation model and computation time

We present here a model that can be used for all types of vehicles to transport hydrogen, except when several consumers can be delivered in the same delivery circuit (which leads to much more complex problems of vehicle routine problem (VRP), which is described in (Toth et Vigo 2014). We will use the generic name "facility" to describe the float of transportation.

We model the batches by two snapshot flow graphs overlaid (see Figure 2 and Figure 3):

- The first one (facility snapshot graph) describes the number of vessels loading, traveling to departure and arrival, unloading and trip back. The variables associated are integer.
- The second one (flow snapshot graph) describes the quantities of hydrogen loaded in the vessel, transported, unloaded. These quantities are limited by the first graph.

From this model, we can also deduce the total number of facilities used at the same time (and optimize it), the fuel consumption and the associated costs.

The facility snapshot graph contains the integer variables:

- $\boldsymbol{P_t}$ is the number of facilities not used between t and $t+1$
- $\boldsymbol{D_t}$ is the number of facilities in charge
- $\boldsymbol{Q_t}$ is the number of facilities travelling from producer to consumer, starting at t
- $\boldsymbol{R_t}$ is the number of facilities coming back, starting at t
- $\boldsymbol{A_t}$ is the number of facilities discharging at t.

As it is a flow graph, the flow have to respect Kirchoff law, all the year long, in departure

$$\boldsymbol{P_{t-1} + D_{t-1} + R_{t-t_{aj}} = P_t + D_t + Q_t} \quad (3)$$

$$\boldsymbol{A_{t-1} + Q_{t-t_{aj}} = A_t + R_t} \quad (4)$$

And the flow snapshot graph is described by the variables:

- $\boldsymbol{u_t}$ the speed of flow (in kg/h) entering in facilities at t
- $\boldsymbol{d_t}$ the quantity of H2 stored in departure between t and $t+1$
- $\boldsymbol{q_t}$ the quantity of H2 sent from departure at t
- $\boldsymbol{a_t}$ the quantity of H2 stored in arrival between t and $t+1$
- $\boldsymbol{e_t}$ the speed of flow delivered to the next component at t

The variables $\boldsymbol{u_t}$ and $\boldsymbol{e_t}$ are the interface variables used to be linked with other models.

https://doi.org/10.52202/077185-0094

With the following Kirchoff constraint:

$$\boldsymbol{u_t} * \Delta t + \boldsymbol{d_{t-1}} = \boldsymbol{d_t} + \boldsymbol{q_t} \quad (5)$$

$$\boldsymbol{q_{t-t_{aj}}} + \boldsymbol{a_{t-1}} = \boldsymbol{e_t} * \Delta t + \boldsymbol{a_t} \quad (6)$$

The graphs are linked together by the capacity C of facilities.

$$\boldsymbol{d_t} \leq C * \boldsymbol{D_t} \quad (7)$$
$$\boldsymbol{q_t} \leq C * \boldsymbol{Q_t}$$
$$\boldsymbol{a_t} \leq C * \boldsymbol{A_t}$$

And the total number of facilities $\boldsymbol{S_{TR}}$ is computed by the two following equations:

$$\boldsymbol{S_{TR}} \geq \boldsymbol{S_{TR_t}} \; \forall t \in \mathcal{Y}$$

$$\boldsymbol{T_{TR_t}} = \boldsymbol{D_t} + \boldsymbol{A_t} + \sum_{i=[0..t_{aj}-1]} \boldsymbol{Q_{t-i}} + \boldsymbol{R_{t+t_{aj}-1-i}} \quad (8)$$

Note that this model allows representing several destinations with a common fleet to optimize.

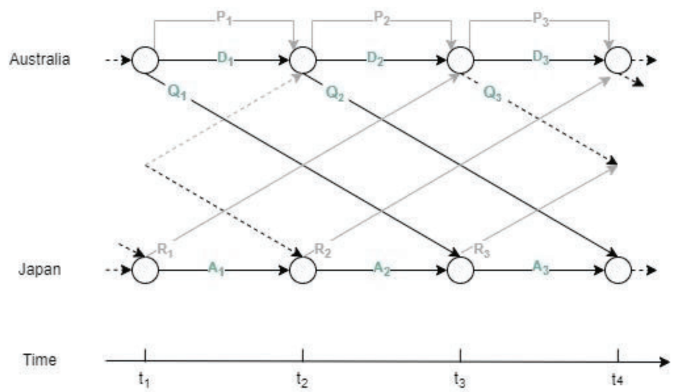

Figure 2 - Snapshot graph of the batches of facilities. All the variables are integer. Variables in blue exists in the flow graph. For instance, Q_1 corresponds to the number of facility starting their journey in Australia at t_1.

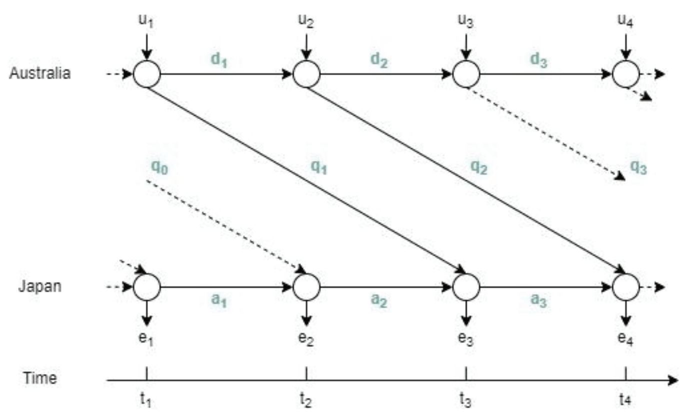

Figure 3 - Snapshot used to model the fluxes. Variables in blue correspond to the ones that exist in the two overlaid graphs. For instance, q_1 corresponds to the quantity of hydrogen in the vessels starting their journey in Australia at t_1.

This model has the advantage to give a realistic view of how the fleet is managed, and to optimize it at the same time as the other components. However, it implies a high number of integer variables. This

https://doi.org/10.52202/077185-0094

leads to high computation times (more than one day to plan a year). For a single optimization, this could be acceptable. Nevertheless, the objective of the project was to perform bi-objective optimization using an evolutionary algorithm. For that purpose, computation times needed to be shorter. We developed two methods to drastically reduce the number of integer variables and consequently reduce the computation times. The first one is the time aggregation (4.2) and the second one the template (4.3).

4.2 Time aggregation and its impacts on computation times

Temporal aggregation is often used to reduce the amount of input data and reduce computation times. Nevertheless, it is applied to the time series for renewable productions or energy demand most of the time (M. Hoffman et al. 2021). In our case, the long computation time is due to the transport module: without considering the vessels computation time is about one minute for the entire supply chain; integrating the complexity of vessels logistic leads to computation times in the order of one day. The objective is then to reduce the number of integer variables for the transportation module.

The principle of time aggregation is to use different time steps for the whole energy system and for a specific component. We aggregate the variables differently if they are flow or stock variables.

Flow variables v and stock variables s are linked together as follows:

$$s_{t+1} - s_t = v_t * \Delta t \tag{9}$$

We name A_g an aggregation, with T_g the number of the model time steps Δt aggregated in the time step Δt_g of A_g. A flow variable v is aggregated as follows in v' :

$$v'_{t_g} = \frac{\sum_{i=0}^{T_g-1} v_{t_g*T_g+i}}{T_g} \tag{10}$$

The reverse operation, to write constraints between aggregated variables and non-aggregated, will be written as follows:

$$v_t = v_{\left\lfloor \frac{t}{T_g} \right\rfloor} \tag{11}$$

Note that if we aggregate an integer variable, it is possible to impose the aggregated variable to be integer, which is more constraining but ensures that it remains integer when de-aggregated.
Stock s_t variables are aggregated in s'_{t_g} as follows:

$$s'_{t_g} = s_{t_g*T_g} \tag{12}$$

And the reverse operation:

$$s_t = s'_{\left\lfloor \frac{t}{T_g} \right\rfloor} \tag{13}$$

In our case study, we applied time aggregation to the transport. The variables $\boldsymbol{q_t}$ of flux departures represent a storage that is shipped at one time step. By aggregating, we reduce the number of possible times of departure to keep the one corresponding to the new time step:

$$q_t = q'_{\frac{t}{T_g}} \text{ if } t \text{ divides } T_g, 0 \text{ else} \tag{14}$$

In our case study, the time step for the complete supply chain is two hours and we choose a time step of 16 hours for shipping. Figure 4 presents a schematic view of the time-step aggregation for vessels.

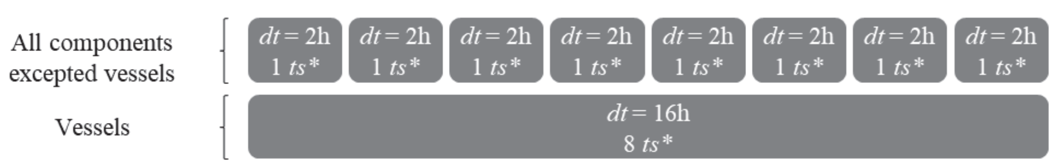

Figure 4 – schematic view of time step aggregation for Vessels

https://doi.org/10.52202/077185-0094

In the case presented in Figure 4, a ship can leave Australia only every 16 hours. The number of integer variables is then reduced by a factor of 8. This method could be used for all other components if needed.

The Table 1 shows the impacts of time aggregation method on resolution times and total costs. Technical costs are evaluated in one MILP optimization including the transport method. The solver used is CPLEX (v 20.1), with a computer with 2 processors Intel Xeon CPU 2.993GHz and 96.0 GB of RAM. The gap is set to 5% to ensure a convergence at a time step of 2 hours without aggregation method. The number of thread is caped to 8.

Table 1 – Impacts of time aggregation method on resolution times and total costs

Time step for the complete supply chain	Time steps for shipping	Resolution times	Total technical costs	Number of vessels *T*	NH_3 Storage size
2 h	2 h	82,659 s		3	
2 h	16 h	3,213 s	+0.4%	4	-42%

As presented in the Table 1, the time aggregation method allows in our case to obtain computation times reduced by more than 25. This method degrades slightly the economic results with a total costs increase of 0.4%. With the aggregation method, there is one more vessel and smaller NH_3 storages.

4.3 Template method

The template method consists in choosing a period Y_p of size T_p which is repeated over the years. Each period of the template is named u_i, $i \in 1..n$. For instance, we choose a period of one month replicated 12 times to model one year.
Instead of using $|Y|$ binary variables v_t to model a decision over time, we use $\left|Y_p\right|$ variables $v_k{}'$.

$$v_t = v_k', k = t \bmod T_p \tag{15}$$

This method adds constraints to the system. The seasonality of the renewable production in Australia is balanced by NH_3 storages in Australia and Japan. Vessels roundtrips are then periodic all along the year. This point can be more realistic than a complete optimized planning with a lot of irregularity.

4.4 Combination of the two methods

Figure 5 shows an illustration of the two combined methods. Note that these two methods can be used for some specific variables of the problem, and not for all of them. It allows mixing efficiently several systems that have to be managed at different timescales. In our case, the vessels use the transport model which needs at least three integer variables by time step.

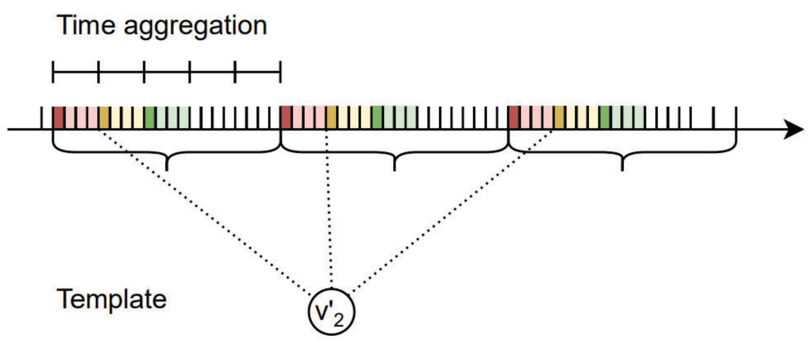

Figure 5 - Example of combination of time aggregation and template method used for the same variable. The coloration represents aggregation of time step, and the brace the same template period repeated over the time.

https://doi.org/10.52202/077185-0094

Figure 6 illustrates the template method for a chosen period of one month.

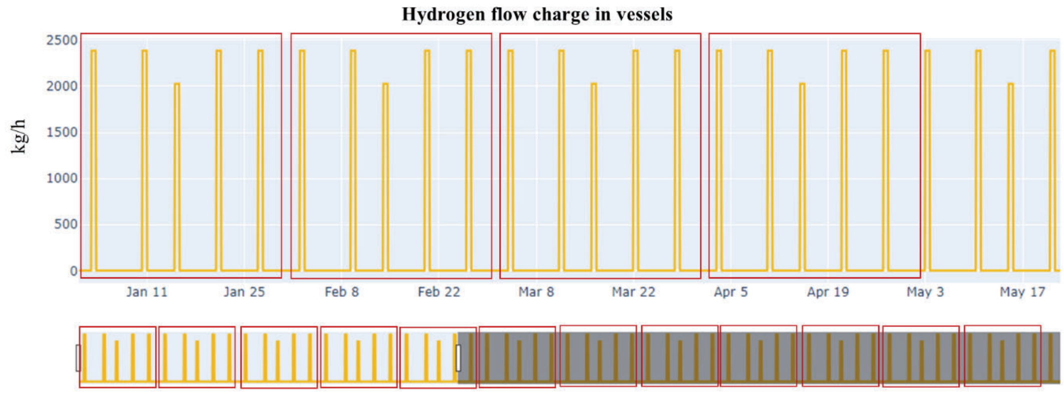

Figure 6 – Illustration of the template method on vessels management.

As shown in Figure 6Figure 6 – Illustration of the template method on vessels management., a given template is replicated every 732 hours. The Table 2 presents the impacts of the combination of the two methods on the resolution time and on the total technical costs.

Table 2 – Impacts of the template method on computation times

Time step for the complete supply chain	Template	Time steps for shipping	Resolution time	Total technical costs	Number of vessels *T*
2h		16 h	3213 s	reference with time aggregation[1]	4
2h	1 month (732 h)	16 h	106 s	+0.0%	4
2h	3 months (2,196 h)	16 h	193 s	+0.67%	4
2h	6 months (4,392 h)	16 h	237 s	+0.67%	4

As shown in Table 2, the template method coupled with time aggregation for shipping allows to obtain resolution times under 250 seconds. The computation time reduction is then 13 times lower than with aggregation time for transportation only, and 330 times lower in comparison with the MILP model without reduction time methods. The impacts on total costs are limited and not significant with an increase of 0.67% of the total technical costs. The choice of the period for the template depends on the optimization period. In our case study, a vessel needs at least 17 days for a roundtrip. Consequently, the minimal used period should be over 17 days.

The obtained computation times are small enough to conduct the bi-objective optimization coupling the MILP solver and an evolutionary algorithm. It allows also to reduce the gap to 0.5%.

5 BI-OBJECTIVE OPTIMIZATION

5.1 Parametric study on carbon emissions

The parametric sensitivity study on carbon emissions consists in minimizing the total costs under carbon emissions constraints. The first run is done without any constraint on CO2 emissions. For the following runs, the emission constraint is reduced from a constant step in absolute value equivalent to about 1% decrease until there is no convergence. We obtain 27 solutions in 439 minutes. The Figure 7 presents the total costs (on the top) and the renewable installed capacities (on the bottom) for each run (report 0 = reference, report 26 = highest carbon emissions constraints that is lowest carbon emissions).

[1] Second line of table 1.

https://doi.org/10.52202/077185-0094

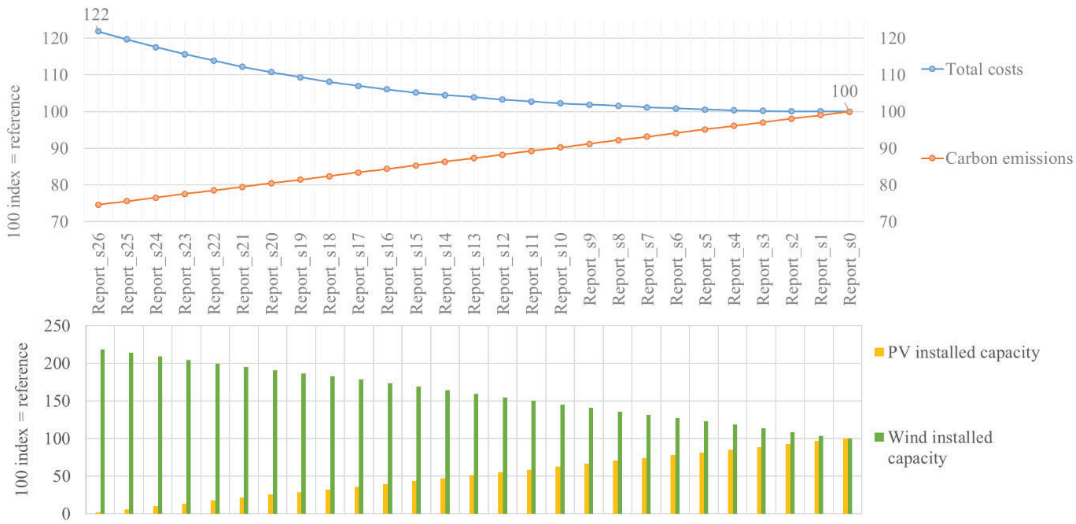

Figure 7 – Parametric study on carbon emissions: total costs (top figure) and renewable capacity installed according to carbon emissions constraints (bottom figure). Report 26: highest constraint, report 0 = reference

As shown on the Figure 7, a 25% decrease of carbon emissions is possible. The impact on total costs is then an increase of 22%. The main factor that allows to decrease carbon emissions is the reduction of installed PV capacity and the increase of wind capacity. Regarding the costs, the wind/PV ratio has no impact (Figure 8). The main component influencing the costs increase is the hydrogen storage which size increases with wind source increase in order to compensate the intermittency.

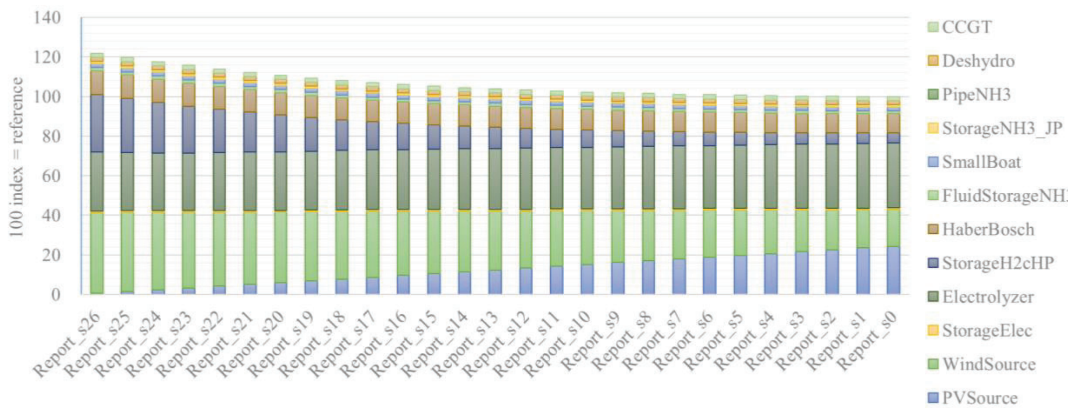

Figure 8 – Parametric study on carbon emissions: total costs breakdown. Report 26: highest CO_2 constraint, report 0 = reference

5.2 Bi-objective optimization

The bi-objective optimization is based on the hybridization of the MILP model with an evolutionary algorithm. The two objective functions used by the loop external to PERSEE are the minimization of the total costs (1) and the minimization of CO2 emissions (2). In order to avoid infeasible solutions we chose to limit the components sized by the external loop to one decisive element of the supply chain and to non-linear elements. The parametric study showed that the wind / PV mix is decisive for the carbon emission criterion. Exploring the complete range of PV or wind installed capacity allow to explore all the possible solutions. Moreover, the advantage of evolutionary algorithm is the capacity to deal with non-linearity. In order to test this ability, the vessels size is optimized by the external loop while the MILP model optimizes the size of the fleet. The MILP model is also in charge of operation

https://doi.org/10.52202/077185-0094

and sizing of all other components (wind power plant, battery, electrolyzer, hydrogen storage, Haber Bosch, ammonia storages, number of vessels, dehydrogenation and the CCGT). We chose to stop the evolutionary algorithm after 30 solutions in the Pareto front.

The 30 solutions in the Pareto front are obtained in 1,065 minutes. Figure 9 presents the total costs (on the top) and the renewable installed capacities (on the bottom) for each solution in the Pareto front.

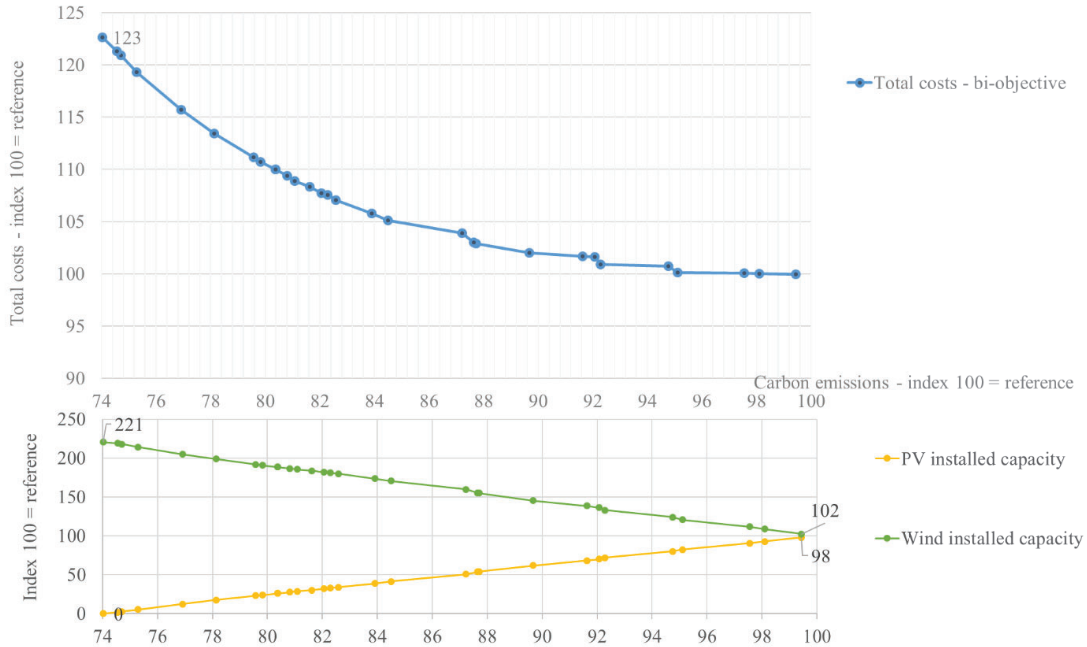

Figure 9 – bi-objective costs – emissions optimization: total costs (top figure) and renewable capacity installed according to carbon emissions (bottom figure). report 0 of parametric study = reference

As shown in Figure 9, a decrease of 26% of carbon emissions should be possible with a cost increase of 23%. The carbon emissions decrease is mainly due to the increase of wind installed capacity and the decrease of PV installed capacity.

5.3 Comparison of parametric study and bi-objectives optimization

The resulting Pareto optimal solutions are then compared to the Pareto optimal solutions computed in Figure 10.

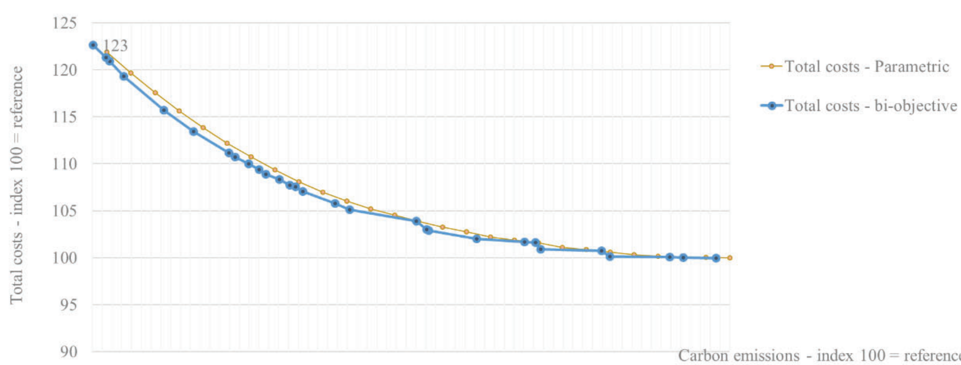

Figure 10 – Comparison of Pareto fronts obtained with a parametric study and with a bi-objectives optimization

https://doi.org/10.52202/077185-0094

The Pareto front of the bi-objective study is slightly under the Pareto front of the parametric study because the vessels size is optimized for the bi-objective study while it is not the case for the parametric study. Figure 10 illustrates also the impact of the step used for the emission constraints in the parametric study: the last step (below index 74) has not converged and we did not obtain the solution for a minimal carbon emission.

The hybridization of MILP model with an evolutionary algorithm allows to:

- (i) run bi-objective optimizations and, at the same time, deal with non-linearity.
- (ii) overcome the steps issue specific to a parametric study.

6 CONCLUSION

The present work presents a MILP model for overseas batch transportation and two methods to drastically reduce the computation time. This will allow to investigate other energy systems with logistics issues. The time aggregation applied to variables of a particular component allows to deal with different time scales. For instance in our case study, the intermittency of renewable production and the longer travelling time for vessels. This could be applied to other components of a supply chain since there is a discrepancy between time scales of components.

The study also illustrates the ability to combine a MILP model with an evolutionary algorithm to deal with non-linearity and multi-objective analysis. The comparison between the parametric study and the bi-objective optimization showed that the Pareto Fronts are quite similar with both methods. The parametric study is less time consuming (more than 2 times less consuming) than the bi-objective method. Nevertheless, the latter allows to take into account non linearity that are arduous to take into account with the MILP approach.

NOMENCLATURE

All variables are written in ***bold*** *and integers ones are in caps.*

Global problem

Set and indices:

$i \in \mathcal{I}$	Components of the system (Solar power plant (PV), Wind power plant (WP), Electrolyzer €, H2 tank (TH2), H2 compressor (CH2), Haber-Bosch (HB), Transportation (TR))
$t \in \mathcal{Y}$	Time steps of the year (hours)

Parameters

c_i	unitary capex of component i
o_i	unitary opex of component i
$p_{i,t}$	economic costs associated to control of component i
g_i	unitary grey emission of component i
$d_{i,t}$	C02 emissions associated to control of component i

Variables

$\boldsymbol{S_i}$	size of component i
$\boldsymbol{v_{i,t}}$	control of component i

Transport model part

Parameters

C	Capacity of one truck
D	Distance between departure and arrival (here Australia and Japan)
sp	speed of a vessel
t_{aj}	Number of time steps to travel between Australia and Japan

https://doi.org/10.52202/077185-0094

Variables

$\boldsymbol{P_t}$	number of facilities not used between t and $t+1$
$\boldsymbol{D_t}$	number of facilities in charge
$\boldsymbol{Q_t}$	number of facilities travelling from producer to consumer, starting at t
$\boldsymbol{R_t}$	number of facilities coming back, starting at t
$\boldsymbol{A_t}$	number of facilities discharging at t
$\boldsymbol{u_t}$	speed of flow (in kg/h) entering in facilities at t
$\boldsymbol{d_t}$	quantity of H2 stored in departure between t and $t+1$
$\boldsymbol{q_t}$	quantity of H2 sent from departure at t
$\boldsymbol{a_t}$	quantity of H2 stored in arrival between t and $t+1$
$\boldsymbol{e_t}$	speed of flow delivered to the next component at t

7 REFERENCES

Blanchard, Jean-Baptiste, Guillaume Damblin, Jean-Marc Martinez, Gilles Arnaud, et Fabrice Gaudier. 2019. « The Uranie Platform: An Open-Source Software for Optimisation, Meta-Modelling and Uncertainty Analysis ». *EPJ Nuclear Sciences & Technologies* 5: 4. https://doi.org/10.1051/epjn/2018050.

Cuisinier, Étienne, Pierre Lemaire, Bernard Penz, Alain Ruby, et Cyril Bourasseau. 2022. « New rolling horizon optimization approaches to balance short-term and long-term decisions: An application to energy planning ». *Energy* 245 (avril): 122773. https://doi.org/10.1016/j.energy.2021.122773.

Efthymiadou, Margarita E., Vassilis M. Charitopoulos, et Lazaros G. Papageorgiou. 2024. « Optimal hydrogen infrastructure planning for heat decarbonisation ». *Chemical Engineering Research and Design* 204 (avril): 121-36. https://doi.org/10.1016/j.cherd.2024.02.028.

Heuser, Philipp-Matthias, D. Severin Ryberg, Thomas Grube, Martin Robinius, et Detlef Stolten. 2019. « Techno-Economic Analysis of a Potential Energy Trading Link between Patagonia and Japan Based on CO2 Free Hydrogen ». *International Journal of Hydrogen Energy* 44 (25): 12733-47. https://doi.org/10.1016/j.ijhydene.2018.12.156.

Hong, Xiaodong, Vaishali B. Thaore, Iftekhar A. Karimi, Shamsuzzaman Farooq, Xiaonan Wang, Adam K. Usadi, Bryan R. Chapman, et Robert A. Johnson. 2021. « Techno-Enviro-Economic Analyses of Hydrogen Supply Chains with an ASEAN Case Study ». *International Journal of Hydrogen Energy* 46 (65): 32914-28. https://doi.org/10.1016/j.ijhydene.2021.07.138.

Kamiya, Shoji, Motohiko Nishimura, et Eichi Harada. 2015. « Study on Introduction of CO2 Free Energy to Japan with Liquid Hydrogen ». *Physics Procedia* 67: 11-19. https://doi.org/10.1016/j.phpro.2015.06.004.

Riera, Jefferson A., Ricardo M. Lima, et Omar M. Knio. 2023. « A review of hydrogen production and supply chain modeling and optimization ». *International Journal of Hydrogen Energy* 48 (37): 13731-55. https://doi.org/10.1016/j.ijhydene.2022.12.242.

Toth, Paolo, et Daniele Vigo. 2014. « Vehicle RoutingProblems, Methods, and Applications ». In *Vehicle Routing*, i-xviii. MOS-SIAM Series on Optimization. Society for Industrial and Applied Mathematics. https://doi.org/10.1137/1.9781611973594.fm.

https://doi.org/10.52202/077185-0094